Am J Physiol Renal Physiol 287: F442–F451, 2004.
First published May 12, 2004; 10.1152/ajprenal.00115.2004.

Functional map of TEA transport activity in isolated rabbit renal proximal tubules

Stephen H. Wright,[1] Kristen K. Evans,[1] Xiaohong Zhang,[1] Nathan J. Cherrington,[2] Daniel S. Sitar,[3] and William H. Dantzler[1]

Departments of [1]Physiology and [2]Pharmacology and Toxicology, University of Arizona, Tucson, Arizona 85724; and [3]Departments of Pharmacology/Therapeutics and Internal Medicine, University of Manitoba, Winnipeg, Canada R3E 0W3

Submitted 1 April 2004; accepted in final form 3 May 2004

Wright, Stephen H., Kristen K. Evans, Xiaohong Zhang, Nathan J. Cherrington, Daniel S. Sitar, and William H. Dantzler. Functional map of TEA transport activity in isolated rabbit renal proximal tubules. *Am J Physiol Renal Physiol* 287: F442–F451, 2004. First published May 12, 2004; 10.1152/ajprenal.00115.2004.—The organic cation (OC) transporters OCT1 and OCT2 are suspected of mediating substrate entry from the blood into proximal tubule cells as the first step in renal secretion of OCs. We examined the contribution of each process in different rabbit renal proximal tubule (RPT) segments, taking advantage of the fact that rabbit orthologs of OCT1 and OCT2 can be distinguished by the high affinity of the former for tyramine (TYR) and of the latter for cimetidine (CIM). We verified that TEA uptake, for which both transporters share a similar affinity, is relatively constant in all three segments (apparent inhibitory constant of 33, 74, and 30 μM and maximal rate of mediated TEA uptake of 0.8, 1.0, and 1.2 pmol·mm^{-1}·min^{-1} in S1, S2, and S3, respectively). In the S1 segment, TYR was a more effective inhibitor of TEA uptake than CIM (IC_{50} values of 39 and 328 μM, respectively), implicating OCT1 as the predominant pathway for TEA transport. The opposite profiles were noted in the S2 segment (IC_{50} values of 302 and 20 μM for TYR and CIM, respectively) and S3 segment (IC_{50} values of 2,900 and 54 μM for TYR and CIM, respectively), suggesting that OCT2 is the predominant TEA transporter in the later portion of RPT. TEA sufficient to saturate OCT1 and OCT2 blocked only 37% of mediated amantadine transport in the S2 segment, confirming the functional presence of at least one additional OC transporter (perhaps OCT3). These data indicate that renal OC transport involves the concerted activity of a suite of transport processes.

organic cation; cimetidine; kidney; organic cation transporter 1; organic cation transporter 2; tetraethylammonium

ORGANIC CATIONS (and weak organic bases; collectively, OCs) are a chemically diverse group of compounds that include a large array of molecules of physiological, pharmacological, and toxicological importance (24). In particular, drugs from a broad array of clinical classes, including antiarrhythmics, β-adrenoreceptor-blocking agents, antihistamines, antivirals, and skeletal muscle relaxing agents, are OCs. The kidney plays a critical role in clearing OCs from the blood, and within the kidney the proximal tubule is the principal site of active OC secretion (18). Secretion of so-called "type I" OCs (i.e., comparatively hydrophilic, monovalent cations with a molecular weight of typically <400; a class of compounds for which tetraethylammonium, TEA, is generally viewed as being representative; see Ref. 14) by proximal tubule cells is a two-step process believed to involve facilitated electrogenic entry of OCs across the basolateral membrane followed by efflux across the luminal membrane mediated by electroneutral exchange of intracellular OCs for intraluminal H^+ (9). Consequently, basolateral OC entry is generally driven by the inside negative membrane potential of proximal tubule cells, whereas OC exit is driven by a transmembrane electrochemical gradient for H^+. Although in this scheme the OC/H^+ exchanger is the active step in transepithelial OC secretion (because of its reliance on an inwardly directed electrochemical gradient for H^+), the overall process of secretion is ultimately reliant on the activity of the Na^+-K^+-ATPase and its role in maintaining the inside negative membrane potential (thereby influencing electrogenic basolateral OC entry) and the Na^+ gradient that drives activity of the Na^+/H^+ exchanger (that, in turn, drives luminal OC/H^+ exchange).

The first step in tubular secretion of OCs, i.e., uptake from the blood into the cell across the basolateral membrane, is suspected to involve interaction with an OC transport pathway. Although physiological evidence has been consistent with the activity of a single mediated process for OCs in the basolateral membrane of proximal cells (e.g., Ref. 21), it is now evident that multiple transporters with similar functional properties but different (though overlapping) specificities can be expressed by renal proximal tubule (RPT) cells. The first of these, OCT1, was cloned from rat kidney in 1994 (6) and subsequently identified in a variety of species, including the human (25). OCT2 was cloned in 1996 (17) and OCT3 in 1998 (13) from rat kidney and placenta, respectively, and subsequently cloned in the human (4, 7) and other species as well (22). All three OCTs display the physiological fingerprint of basolateral OC transport in that they support electrogenic transport of TEA and other OCs (22). OCT1 has been shown by immunocytochemistry to be expressed in the basolateral membrane of rat proximal tubule cells (12, 15), and OCT2 has been shown to be expressed in the basolateral membrane of both human and rat proximal tubule cells (12, 16); the subcellular distribution of OCT3 in the kidney has not been examined. There is general consensus that basolateral OC transport in the kidney is dominated by activity of OCT1 and OCT2. The comparatively low level of OCT3 expression in the kidney (16, 20), combined with a profile of substrate specificity evident in studies with renal tissue (23), suggests that OCT3 (which was originally referred to as the extraneuronal monoamine transporter; see Ref. 7) may play a minor role in mediating secretion of type I OCs. Further supporting the predominant importance of OCT1

Address for reprint requests and other correspondence: S. H. Wright, Dept. of Physiology, College of Medicine, Univ. of Arizona, Tucson, AZ 85724 (E-mail: shwright@u.arizona.edu).

The costs of publication of this article were defrayed in part by the payment of page charges. The article must therefore be hereby marked "*advertisement*" in accordance with 18 U.S.C. Section 1734 solely to indicate this fact.

and OCT2 in the kidney is the observation that renal uptake and clearance of TEA in OCT1/2(−/−) knockout mice is effectively eliminated (10).

Although the combined influence of OCT1 and OCT2 in renal OC secretion is evident, the relative roles played by each in mediating the entry step in OC secretion by the proximal tubule are not clear. In the rat, although OCT1 and OCT2 are both expressed in RPT cells, there is a marked axial heterogeneity in the expression of these two proteins along the length of the proximal tubule (12). On the one hand, OCT1 expression is greatest in the S1 (early) segment of RPT and is absent in the S3 (late) segment. OCT2 expression, on the other hand, begins in the S2 (mid) segment of RPT and continues in the S3 segment, and there is clear coexpression of OCT1 and OCT2 in the S2 segment (12). However, in human kidney, an immunocytochemical assessment of the distribution of OCTs clearly documented the basolateral expression of OCT2 but found no evidence of OCT1 expression in RPT (16). Although the marked difference in apparent levels of OCT1 and OCT2 expression in human kidney could, at least in part, reflect differences in antibody immunoreactivity, parallel measurement of mRNA quantified using real-time PCR found that the OCT1 mRNA level in human renal tissue is 1% of that of OCT2 (16). Although these data argue that human renal OC secretion is likely dominated by OCT2, it is evident in other studies that OCT1 is expressed in human renal tissue, albeit at levels substantially lower than OCT2 (4), leading to the suggestion that OCT1 may play a "housekeeping" role in human kidney (4).

It can be difficult, however, to infer the extent to which a transporter contributes to net secretory activity based on relative expression levels of mRNA or immunoreactive protein. We recently assessed the functional contribution of OCT1 and OCT2 to OC transport activity in isolated single S2 segments of rabbit kidney. We found that uptake of TEA, which is transported with similar efficacy by OCT1 and OCT2 orthologs from most species, is dominated by activity of OCT2, and that this is correlated with comparatively low levels of OCT1 mRNA (compared with OCT2; see Ref. 11). Nevertheless, OCT1 supported ~75% of the transport of tyramine (TYR), an "OCT1-selective" substrate, into isolated single S2 segments, underscoring the fact that even low levels of transporter expression can result in a significant contribution to the transport of some substrates.

In the present study, we extend the "functional mapping" of OC transport activity in rabbit RPT to the early and late portions of the tubule, i.e., the S1 and S3 segments. The S1 segment displayed a profile of OCT activity that was virtually the opposite of that expressed in the S2 segment in that TEA transport was dominated by an interaction with OCT1, rather than with OCT2. In contrast, the characteristics of TEA transport into cells of the S3 segment were similar to those of the S2 segment, i.e., transport activity dominated by an interaction with OCT2. Interestingly, the kinetics of net TEA transport was virtually identical in all three segments, despite the different contributions of separate transporters. Finally, the functional presence of at least one other transporter (perhaps OCT3) in rabbit RPT was inferred from the observation that mediated uptake of amantadine was only partially inhibited by concentrations of TEA capable of completely eliminating the contribution of OCT1 and OCT2.

METHODS

Materials. New Zealand White rabbits were purchased from Harlan (Indianapolis, IN). The Chinese Hamster Ovarian cell line, CHO-K1, was purchased from American Type Culture Collection (Rockville, MD). [^{3}H]TEA (20.0 Ci/mmol) was prepared by the Synthesis Core of the Southwest Environmental Health Science Center of the University of Arizona; [^{14}C]TEA (56 mCi/mmol) was prepared by Wizard Labs (Davis, CA). [^{3}H]amantadine (28 Ci/mmol) was prepared by Amersham International (Buckinghamshire, UK). All other chemicals were purchased from Sigma Chemical (St. Louis, MO) or other sources and were generally the highest purity available. Cell culture media and all other molecular biology reagents were purchased from Sigma Chemical or Life Technologies (Gaithersburg, MD).

Transport in isolated rabbit proximal tubule segments. New Zealand White rabbits were killed by intravenous injection with pentobarbital sodium, and all protocols involving rabbits were conducted in accordance with the *Guide for the Care and Use of Animals* as adopted and promulgated by the National Institutes of Health. The kidneys were flushed via the renal artery with an oxygenated ice-cold HEPES-sucrose solution, pH 7.4 (10 mM HEPES and 250 mM sucrose, pH adjusted with Tris base). Transverse slices of an isolated kidney were placed in a dish containing ice-chilled dissection buffer (in mM: 110 NaCl, 25 $NaHCO_3$, 5 KCl, 2 Na_2HPO_4, 1.8 $CaCl_2$, 1 $MgSO_4$, 10 sodium acetate, 8.3 D-glucose, 5 L-alanine, 4 lactate, and 0.9 glycine; adjusted to pH 7.4 with HCl or NaOH and gassed continuously with 95% O_2-5% CO_2 to maintain the pH; osmolarity of ~290 mosmol/kgH_2O). S1, S2, or S3 segments were dissected manually from a kidney slice at 4°C without use of enzymatic digestion. All proximal segments were carefully teased from superficial nephrons. S1 pieces, from 0.35 to 0.75 mm running length, were gently pulled from the curly masses of S1 tubules that surrounded glomeruli typically located slightly below the cortical surface. S2 portions of rabbit RPT were prepared by teasing a 1.0- to 1.3-mm length of straight tubule starting at the cortical surface of the kidney. S3 segments were dissected by pulling out 0.7- to 1.1-mm lengths of straight proximal tubule starting at its junction with the descending thin limb of Henle's loop. Extra caution was taken with S3 segments to be sure that they were not from juxtamedullary nephrons.

Transport studies with single tubule segments were performed in a temperature-controlled chamber at 37°C. Uptakes were measured by transferring each tubule to an oil-covered well in the chamber containing dissection buffer and radiolabeled substrate, with or without inhibitors of interest. After an incubation (of 2 s to 30 min), uptake was stopped by transferring the tubule to a microwell (60-well plate; Nunc, Naperville, IL) containing 7 μl of 1 N NaOH covered with light mineral oil. The tubules were solubilized for at least 30 min, after which the tubule extracts were transferred to small scintillation vials containing 200 μl distilled water. Scintillation cocktail (3 ml) was added to each vial, and the radioactivity was determined using liquid scintillation spectroscopy. At least three tubules were used to determine transport for each experimental condition tested. Transport rates were normalized to tubule length based on measurements derived from photographs taken through a dissecting microscope equipped with a digital image capture system (Snappy; Play). Data are presented as means ± SE or, in some cases, SD. To facilitate comparison of these data obtained using intact tubules with those measured in other cell systems, we offer a rough conversion factor, i.e., ≃0.8 mg protein/mm tubule length.

Stable expression of rbOCT1 or rbOCT2 in CHO-K1 cells. CHO-K1 cells were transiently transfected with cDNAs for the rabbit orthologs of either OCT1 (rbOCT1) or OCT2 (rbOCT2) and after 24 h placed in culture medium supplemented with 1 mg/ml G-418 (GIBCO-BRL). Surviving cells were tested for the functional expression of OC transport activity by using the fluorescent OC [2-(4-nitro-2,1,3-benzoxadiazol-7-yl)aminoethyl]trimethylammonium (NBD-TMA), which has been shown to be a substrate for peritubular OC transport in single isolated rabbit RPTs (1). Single colonies that

accumulated 20 μM NBD-TMA were selected from 96-well plates. Stable clonal cell lines that expressed either rbOCT1 or rbOCT2 were grown in the selection medium and used for subsequent experiments.

Transport in cultured cells. Uptake of [^{3}H]TEA in cells expressing either rbOCT1 or rbOCT2 was measured at 25°C. After the culture media were removed, confluent cell monolayers were washed two times with Waymouth's buffer (WB; in mM: 135 NaCl, 13 HEPES, 28 D-glucose, 5 KCl, 1.2 $MgCl_2$, 2.5 $CaCl_2$, and 0.8 $MgSO_4$, pH adjusted to 7.4 with NaOH) and then preincubated for a total of 30 min in WB (2 × 15 min). The transport buffer consisted of WB containing radiolabeled substrate with or without test inhibitors. Uptake was stopped by removing the transport buffer and then rinsing the cells with three successive washes with 1 ml ice-cold WB containing 250 μM tetrapentylammonium. The cells were solubilized with 1% SDS in 0.2 N NaOH, neutralized with 0.4 N HCl, and transferred to scintillation vials to measure accumulated radioactivity (Beckman LS 3801; Beckman instruments, Irvine, CA). Uptake rates are expressed as moles per square centimeter of surface area of the confluent monolayer.

Isolation of rabbit OCT3. A partial rbOCT3 sequence was obtained from GenBank (accession no. AF294824). Two gene-specific primers, 5′-GGCTGATCACTCGGAAGGAA-3′ (sense) and 5′- AGTATAAGGGTGCACTTCCTCA -3′ (antisense), were designed from the partial rbOCT3 sequence for 5′- and 3′-rapid amplification on cDNA ends (RACE), as described previously (26). Briefly, both the 5′- and the 3′-RACE reactions were primed with an internal gene-specific primer and an adaptor primer. The PCR reactions were performed according to the manufacturer's protocols. The RACE products were gel purified and subcloned into the mammalian expression vector pcDNA3.1. The two overlapped PCR fragments were reconstructed as full-length rbOCT3 in pcDNA3.1. Sequences of the two overlapping RACE products were confirmed in both the sense and antisense strands by an Applied Biosystems model 373A sequencing unit at the University of Arizona sequencing facility.

Branched DNA signal amplification assay. OCT mRNA was measured using the branched DNA (bDNA) assay (Quantigene bDNA signal amplification kit) with modifications (8). Rabbit OCT gene sequences of interest were accessed from GenBank (see Table 1). Multiple oligonucleotide probes (containing capture, label, and blocker probes) specific to a single mRNA transcript (i.e., OCT1, -2, or -3) were designed using Probe Designer software version 1.0, with a melting temperature of ~63°C, enabling hybridization conditions to be held constant (i.e., 53°C) during each hybridization step and for each probe set. Every probe developed in Probe Designer was submitted to the National Center for Biotechnological Information (Bethesda, MD) for nucleotide comparison by the basic logarithmic alignment search tool (BLASTn) to ensure minimal cross-reactivity with other known rabbit sequences and expressed sequence tags. The nucleotide sequence and function of these probes are given in Table 1. Total RNA (1 μg/μl; 10 μl/well) was added to each well of a 96-well plate containing 50 μl capture hybridization buffer and 50 μl of the desired probe set diluted in lysis buffer per the manufacturer's protocol. For each gene, total RNA was allowed to hybridize to the probe set overnight at 53°C. Subsequent hybridization steps were carried out according to the manufacturer's protocol, and luminescence was measured with a Quantiplex 320 bDNA luminometer interfaced with Quantiplex Data Management software version 5.02 for analysis of luminescence from the 96-well plates. The luminescence for each well is reported as relative light units per 10 micrograms total RNA.

RESULTS

Molecular properties of rbOCT3. PCR-based 5′- and 3′-RACE resulted in 1113-bp and 1980-bp fragment PCR products, respectively. The full length of rbOCT3 contained 2912 bp, which encoded a 1215-bp open-reading frame (ORF) and a 508-bp 3′-untranslated region. The amino sequence of the ORF (GenBank accession no. AY555578) was 92% identical to the corresponding region of human OCT3. The portion of the nucleotide sequence encoding the ORF was used to generate primers used for the bDNA signal amplification procedure.

OCT mRNA levels in rabbit kidney. Figure 1 compares the mRNA levels determined for OCT1, OCT2, and OCT3 in total RNA isolated from renal cortex collected from male or female rabbits. Two observations are worth noting. First, there was no significant difference in mRNA levels in males vs. females for any of the transporters. This contrasts with studies employing rats that, while showing no sex-based differences in mRNA levels for OCT1 and OCT3, observed a fourfold higher expression of OCT2 mRNA in male rat kidney compared with female rat kidney (20). Sex-based differences in OCT2 mRNA in the rat were, however, only noted in adult rats, and the rabbits used in the present study were ~9.5 ± 1 wk in age, well short of sexual maturity (~16 wk).

The second point pertinent to the present study is the observation that mRNA expression for the three transporters appeared to differ markedly, in the descending order OCT2 >> OCT1 > OCT3, similar to the pattern observed in rat kidney (20). Comparison of the signals obtained with the three probe sets used in the bDNA signal amplification method must be made cautiously because of possible differences in amplification efficiency. However, the presence of multiple hybridization sequences in the probe sets for each transporter reduces problems arising from variable hybridization efficiency (8) and supports the contention that the differences in signal levels between the three transporters evident in Fig. 1 reflect real differences in the relative expression of the three mRNA species.

Kinetics of TEA transport in isolated S1, S2, and S3 segments of rabbit RPT. Figure 2 shows the time course of [^{3}H]TEA uptake (0.8 μM) in single isolated S1 segments of rabbit RPT. Uptake was time dependent over the 30-min course of the experiment, and addition of 2 mM unlabeled TEA reduced this uptake by ~95% at each time point tested. Basolateral uptake of [^{3}H]TEA approached steady state between 20 and 30 min, but over the first 2 min accumulation was near first order. This temporal profile of TEA uptake in isolated S1 segments was similar to that reported previously for basolateral TEA uptake in single isolated S2 segments of rabbit RPT (5). We elected to use 2-min uptakes to provide estimates of the initial rate of TEA uptake in all three segments for two reasons. First, the similarity in the characteristics of TEA uptake in these S1 and S2 segments suggested that uptake in the S3 segment was unlikely to be substantially different (an assumption born out by the subsequent measurement of the kinetics of transport in each segment). Second, incubations of that length were required to provide a sufficient number of radioactive counts to perform kinetic analyses in the comparatively short S1 and S3 segments.

Figure 3 shows the effect of increasing concentrations of TEA on the rate of total TEA uptake in single, nonperfused S1, S2, and S3 segments of rabbit RPT. The kinetic profile of uptake in all three segments was similar and adequately described by the relationship:

Table 1. *Oligonucleotide probes generated for analysis of OCT expression by bDNA signal amplification*

Gene	GenBank ID	Target	Function	Probe Sequence
rbOCT1	AF015958	530–548	CE	ccagggagccgaggaagaaTTTTTctcttggaaagaaagt
		660–677	CE	gcaggcggaagagcagcaTTTTTctcttggaaagaaagt
		823–839	CE	gccagttcgggatggcgTTTTTctcttggaaagaaagt
		860–877	CE	gaggaaggtgggcagggaTTTTTctcttggaaagaaagt
		511–529	LE	gcccaggttcacgcaggacTTTTTaggcataggacccgtgtct
		549–569	LE	tgtctgcgatgtagccgacacTTTTTaggcataggacccgtgtct
		587–606	LE	agggtggtcagcagcagacaTTTTTaggcataggacccgtgtct
		607–624	LE	cccgacaccgcgttgatcTTTTTaggcataggacccgtgtct
		625–641	LE	ccacggccgtgagcaccTTTTTaggcataggacccgtgtct
		642–659	LE	tggacgtgtagtccggcgTTTTTaggcataggacccgtgtct
		692–710	LE	acatccagctgcccttgctTTTTTaggcataggacccgtgtct
		711–730	LE	tgtgatcagggtgtagccggTTTTTaggcataggacccgtgtct
		731–749	LE	agcctgagcccacgaactcTTTTTaggcataggacccgtgtct
		750–767	LE	tggccaccgtcctcctgtTTTTTaggcataggacccgtgtct
		768–787	LE	gaaggccacctggtacaggaTTTTTaggcataggacccgtgtct
		788–805	LE	ggccaccagccccacagaTTTTTaggcataggacccgtgtct
		806–822	LE	taggcgacgcccgagagTTTTTaggcataggacccgtgtct
		570–586	BL	cagcttgcggccaaacc
		678–691	BL	gaccaggccctgca
		840–859	BL	cacagtgagctgcagccagc
rbOCT2	AF458095	1324–1343	CE	acagtgatcctcagcccctgTTTTTctcttggaaagaaagt
		1360–1377	CE	ggccatggtgatccccatTTTTTctcttggaaagaaagt
		1417–1438	CE	caccgagattcctgatgaacgtTTTTTctcttggaaagaaagt
		1511–1527	CE	gggcagctgcagccagaTTTTTctcttggaaagaaagt
		1625–1646	CE	cttggtctctgcaggttttcagTTTTTctcttggaaagaaagt
		1673–1693	CE	cgtctgctttcctaacgtggaTTTTTctcttggaaagaaagt
		1283–1301	LE	gaggctagacacgcagcccTTTTTaggcataggacccgtgtct
		1302–1323	LE	cagatcatcagggacaaacacgTTTTTaggcataggacccgtgtct
		1378–1398	LE	gaccaggcacaccatctcgtaTTTTTaggcataggacccgtgtct
		1439–1457	LE	agcgaggagcagaccaggaTTTTTaggcataggacccgtgtct
		1458–1473	LE	gccgccgacgtcgcacTTTTTaggcataggacccgtgtct
		1493–1510	LE	tggccgtgagccggtagaTTTTTaggcataggacccgtgtct
		1528–1545	LE	caccgcgaacaccaccaaTTTTTaggcataggacccgtgtct
		1546–1563	LE	tcctgccaccaagcccacTTTTTaggcataggacccgtgtct
		1564–1583	LE	ggcagcatcaacaccagtccTTTTTaggcataggacccgtgtct
		1584–1605	LE	caaggttctccctttggtttctTTTTTaggcataggacccgtgtct
		1606–1624	LE	cttcctcgatggtctcgggTTTTTaggcataggacccgtgtct
		1647–1672	LE	cataaatcacctttttctctgttttttTTTTTaggcataggacccgtgtct
		1344–1359	BL	cctgcccaagcaggcc
		1399–1416	BL	ggggtacagctcggcgtt
		1474–1492	BL	ccaggaagggcgtgacgat
rbOCT3		686–704	CE	gcctccaatgatccccaggTTTTTctcttggaaagaaagt
		886–907	CE	cctagtcttcccagggtagcgaTTTTTctcttggaaagaaagt
		1057–1073	CE	cagcgggagctccagccTTTTTctcttggaaagaaagt
		1134–1152	CE	ctggcagggctattcccttTTTTTctcttggaaagaaagt
		733–750	LE	ccggcagctccaccactcTTTTTaggcataggacccgtgtct
		751–770	LE	cagcaagatcaggagcgctcTTTTTaggcataggacccgtgtct
		771–789	LE	gtccaaggcgctcaatggtTTTTTaggcataggacccgtgtct
		807–826	LE	cctgccatcatattgctggcTTTTTaggcataggacccgtgtct
		827–843	LE	tgaccaggcacgccaccTTTTTaggcataggacccgtgtct
		844–864	LE	ccccttctggtaagaacgcagTTTTTaggcataggacccgtgtct
		865–885	LE	ctgtggtcctcaaccacggtaTTTTTaggcataggacccgtgtct
		908–929	LE	gatttcaaaggccatggttatgTTTTTaggcataggacccgtgtct
		930–957	LE	ggtacagttctgaatttaccaaatagacTTTTTaggcataggacccgtgtct
		981–1000	LE	aaacccgaacacagcgagacTTTTTaggcataggacccgtgtct
		1001–1020	LE	tgatgcccccaaaatcacacTTTTTaggcataggacccgtgtct
		1095–1114	LE	acgaggccaccacagacagaTTTTTaggcataggacccgtgtct
		1153–1176	LE	ggttttctacgtcgtccactgtctTTTTTaggcataggacccgtgtct
		705–732	BL	cggagatgaagaagtctatatagaggtt
		790–806	BL	cgcaaaggggaggcgac
		958–980	BL	cccaaagtttcgtaatgttgttg
		1022–1041	BL	ggaagaggaggaaaggggca
		1042–1056	BL	acacggccgccagcc
		1074–1094	BL	cgccaggacaccaaagatgat
		1115–1133	BL	ggtttccggcagaagcatc

OCT, organic cation transporter; bDNA, branched DNA. Target refers to the sequence of the mRNA transcript as enumerated in the GenBank file. Function refers to how the oligonucleotide probe was used in the bDNA assay. CE, capture extender; LE, label extender; BL, blocker probe.

$$J = \frac{J_{cap}[T]}{K_{50} + [T]} + D[T] \quad (1)$$

where J is the rate of TEA uptake from concentration [T]; J_{cap} is the maximal rate of mediated TEA uptake, reflecting the total transport capacity of the membrane (including the potential influence of multiple transport processes); K_{50} is a half-saturation constant; and D is a coefficient that describes the component of total TEA uptake that was not saturable over the concentration range studied (reflecting some combination of diffusion, binding, and/or insufficient rinsing of radiolabel from the tubules). As evident in Fig. 3, the kinetic parameters for basolateral TEA uptake were comparatively similar along the entire length of the rabbit RPT (K_{50} values, in μM, for S1, S2, and S3 of 32.9 ± 9.7, 74.3 ± 19.6, and 29.5 ± 3.1, respectively; J_{cap} values, in pmol·mm^{-1}·min^{-1}, for S1, S2, and S3 of 0.77 ± 0.23, 0.95 ± 0.13, and 1.17 ± 0.26, respectively). Of particular interest is the observation that TEA uptake in each segment was half-saturated by bath concentrations ranging from 20 to 75 μM, values that correlate reasonably well with the Michaelis constants for TEA uptake mediated by the rabbit orthologs of OCT1 and OCT2 when expressed in mammalian cells, i.e., 20 and 35 μM for OCT1 and OCT2, respectively, when expressed in CHO cells; 120 and 75 μM for OCT1 and OCT2, respectively, when expressed in COS-7 cells (11).

Selectivity profiles for the transport processes involved in TEA uptake in the S1, S2, and S3 segments of rabbit RPT. Although rabbit OCT1 and OCT2 have similar affinities for TEA (and a number of other "nondiscriminating" OCs; see Ref. 11), selected compounds discriminate markedly between these homologous transporters. In particular, rbOCT2 shows a 50- to 70-fold higher apparent affinity for cimetidine (CIM) than does rbOCT1, whereas rbOCT1 shows a 12- to 17-fold higher affinity for TYR than does rbOCT2 (11). In previous studies, we used these differences in selectivity to "functionally map" the expression of OCT transporter activity in isolated S2 segments of rabbit RPT (11, 26). Figure 4 is a summary of selected elements of that previous study. It was drawn to permit a direct comparison of the selectivity profile obtained for S2 segments in the previous study with the selectivity profiles obtained for S1 and S3 segments in the current study (shown in Figs. 5 and 6) and to serve as a vehicle for describing the rationale used for these comparisons. Figure 4*A* shows the effect of increasing concentrations of CIM or TYR on basolateral uptake of TEA in isolated single S2 segments. The resulting inhibitions were described by the relationship:

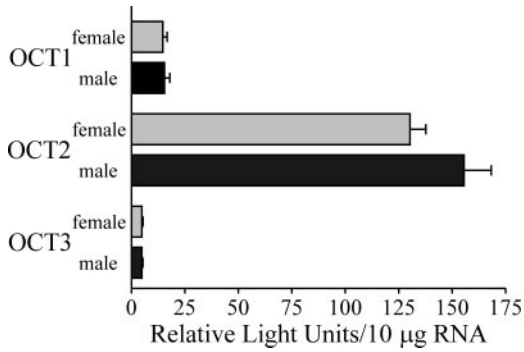

Fig. 1. Relative expression of mRNA for organic cation transporter (OCT) 1, OCT2, and OCT3 in rabbit renal cortical tissue. Cortical total RNA was isolated from 60- to 70-day-old male and female rabbits and analyzed by the branched DNA (bDNA) signal amplification assay for OCT mRNA content. Each bar represents the mean (expressed as relative light units) ± SE determined from tissues isolated from 7 animals.

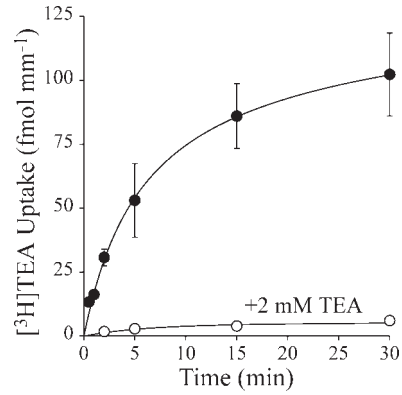

Fig. 2. Time course of [^{3}H]TEA (0.8 ± 0.03 μM) uptake in isolated single S1 segments of rabbit renal proximal tubule (RPT). Uptakes were measured in absence or presence of 2 mM unlabeled TEA. ●, Mean uptakes ± SE, measured in triplicate, in tubules from 5 different rabbits (i.e., $n = 5$). Uptakes measured in the presence of 2 mM TEA (○) were measured, again in triplicate, in 1 or 2 experiments.

$$J^* = \frac{J_{app}[T^*]}{K_{app} + [I]} + C \quad (2)$$

where J^* is the rate of [^{3}H]TEA transport from a concentration of labeled substrate equal to [T*] measured in the presence of inhibitor concentration equal to [I]; J_{app} is defined as (K_i/K_t)J_{max}; K_{app} is an apparent inhibitory constant (K_i) for the test agent that is defined as $K_i(1 + [T^*]/K_t)$ (note: when [T*] is $\ll K_t$, $K_{app} \approx K_i$); and C is a constant equal to the accumulation of T* that appears to be unsaturable. The structure of the relationship outlined in *Eq. 2* assumes that the interaction between T* and I is competitive. In fact, CIM and TYR are both transported by rbOCT1 and rbOCT2 (Ref. 11 and unpublished observations), so the assumption of a competitive interaction between these substrates is reasonable. Nevertheless,

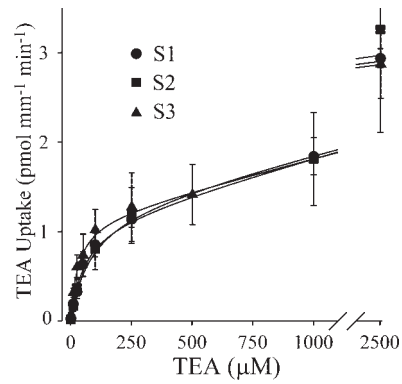

Fig. 3. The kinetics of TEA uptake in single nonperfused segments of rabbit RPT. The initial rate of [^{3}H]TEA (~1 μM) uptake, measured in the presence of increasing concentrations, was estimated from 2-min uptakes. Each point represents the mean of uptakes, measured in triplicate, in tubules collected from 5 rabbits. Kinetics parameters were calculated from nonregression analysis (SigmaPlot 3.0; Jandel Scientific) of these data against the relationship outlined in *Eq. 1*.

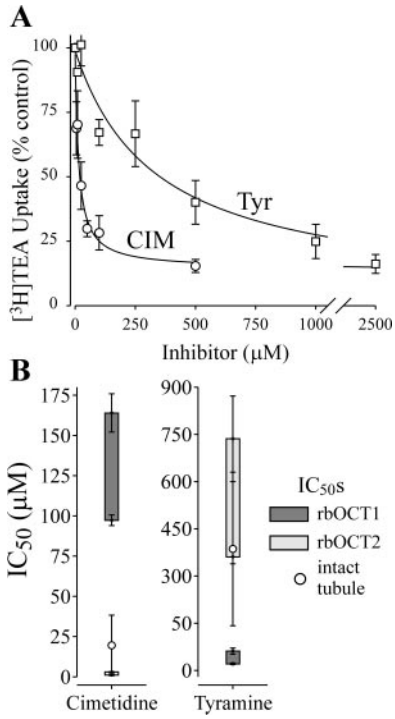

Fig. 4. *A*: kinetics of inhibition of [^{3}H]TEA uptake in isolated single S2 segments of rabbit RPT produced by exposure to increasing concentrations of tyramine (TYR) or cimetidine (CIM). These data are redrawn from Ref. 11 (see text). They were put in this form to facilitate direct comparison of the previous data with the current data shown in Figs. 5 and 6. Rates of TEA uptake were based on 2-min uptakes. Each point is the mean ± SE of uptakes measured in triplicate in tubules isolated from 3 to 5 rabbits. IC_{50} values were calculated from nonregression analysis (SigmaPlot 3.0; Jandel Scientific) of these data against the relationship outlined in *Eq. 2*. *B*: comparison of the IC_{50} values determined for TYR and CIM as inhibitors of TEA uptake in single S2 segments with the IC_{50} values determined for rbOCT1 and rbOCT2 expressed in cultured cells. These data are redrawn from Ref. 11 (see text). They were put in this form to facilitate direct comparison of the previous data with the current data shown in Figs. 5 and 6. The dark gray bars depict the range of IC_{50} values determined for inhibition of rbOCT1 as expressed in either CHO-K1 cells or COS-7 cells. The light gray bars depict the range of IC_{50} values determined for inhibition of rbOCT2, as expressed in either CHO-K1 cells or COS-7 cells. In each case, the higher end of the range (shown as a solid point ± SE) indicates the value determined in COS-7 cells. ○, Mean IC_{50} value ± SD for inhibition of mediated TEA uptake in isolated, single nonperfused S2 segments of rabbit RPT.

inhibitory interactions in the tubules may well reflect the influence of multiple transporters. Consequently, we generally refer to the kinetic constants derived from use of *Eq. 2* (measured in both tubules and cultured cells) as "IC_{50} values." In the S2 segment, the IC_{50} (i.e., K_{app}) values for TYR and CIM were 302 and 20 μM, respectively (Fig. 4*B*). The kinetic values obtained in intact tubules are compared in Fig. 4 with the IC_{50} values reported previously (11) for CIM and TYR as inhibitors of TEA transport mediated by rabbit OCT1 and OCT2, as expressed in cultured CHO and COS-7 cells. It is appropriate to emphasize that these IC_{50} values were not identical in the two cell types, and this is indicated graphically in Fig. 4*B*: the dark shaded bars represent the range of IC_{50} values (±SE) obtained for CIM and TYR inhibition of TEA transport that was mediated by rbOCT1; the range of IC_{50} values (±SE) for CIM and TYR inhibition of TEA transport mediated by rbOCT2 is shown. For both transporters, the lower IC_{50} values within each range were obtained using CHO cells, whereas the higher values reflect transport in COS-7 cells. As reported previously (11), the comparatively low IC_{50} for CIM inhibition of TEA uptake in intact S2 segment combined with the comparatively high IC_{50} for TYR inhibition of TEA uptake support the conclusion that OCT2 is primarily responsible for the basolateral transport of TEA within the S2 segment of rabbit RPT.

Figure 5 shows the profile of inhibition of TEA uptake in single isolated S1 segments of rabbit RPT produced by CIM and TYR. Interestingly, the pattern of inhibition of TEA uptake in the S1 segment produced by these two compounds was the opposite of that observed in the S2 segment, as described above. In the S1 segment, the IC_{50} for TYR inhibition of TEA uptake was 39.1 ± 8.4 μM (Fig. 5*A*), which was within the range of IC_{50} values observed for interaction with rbOCT1 (Fig. 5*B*). If TEA transport in the S1 segment was dominated by activity of OCT1, then CIM should have been a comparatively poor inhibitor of TEA uptake. This was, indeed, the case: the IC_{50} for CIM inhibition of TEA uptake in the S1 segment was 328 ± 108 μM, a value profoundly different from the 1- to 3-μM IC_{50} for inhibition of rbOCT2 in cultured cells, and similar to CIM's weak inhibition of rbOCT1 (360–740 μM; see Ref. 11). These observations support the conclusion that TEA uptake in the S1 segment of rabbit RPT occurred predominantly via OCT1.

Figure 6 shows the profile of inhibition of TEA uptake in single isolated S3 segments of rabbit RPT produced by CIM

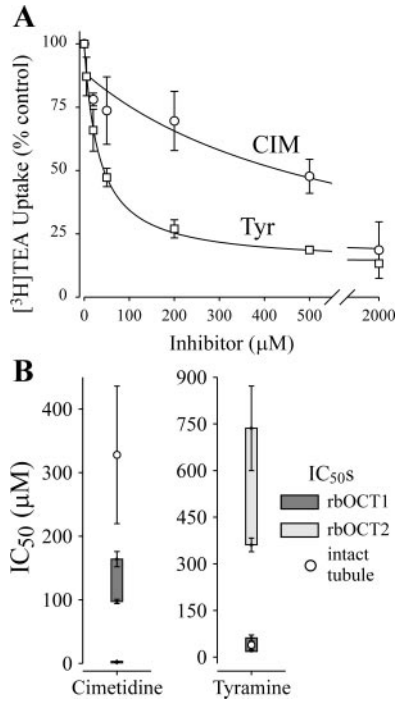

Fig. 5. *A*: kinetics of inhibition of [^{3}H]TEA uptake in isolated single S1 segments of rabbit RPT produced by exposure to increasing concentration of TYR or CIM. Rates of TEA uptake were based on 2-min uptakes. Each point is the mean ± SE of uptakes measured in triplicate in tubules isolated from 6 to 7 rabbits. *B*: comparison of the IC_{50} values determined for TYR and CIM as inhibitors of TEA uptake in single S1 segments with the IC_{50} values determined for rbOCT1 and rbOCT2 expressed in cultured cells (details as in Fig. 4). ○, Mean IC_{50} value ± SD for inhibition of mediated TEA uptake in isolated, single nonperfused S1 segments of rabbit RPT.

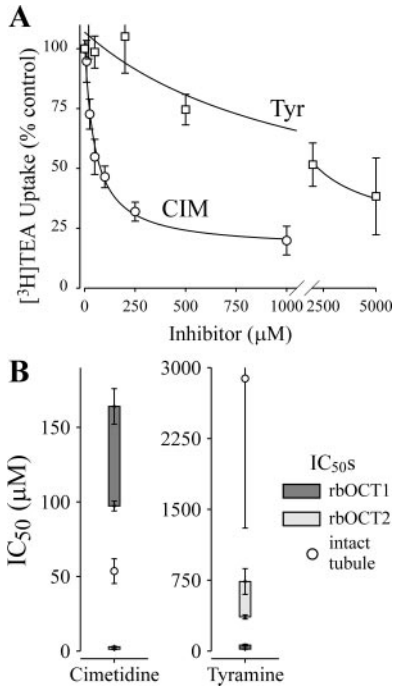

Fig. 6. *A*: kinetics of inhibition of [^{3}H]TEA uptake in isolated single S3 segments of rabbit RPT produced by exposure to increasing concentration of TYR or CIM. Rates of TEA uptake were based on 2-min uptakes. Each point is the mean ± SE of uptakes measured in triplicate in tubules isolated from 5 rabbits. *B*: comparison of the IC_{50} values determined for TYR and CIM as inhibitors of TEA uptake in single S3 segments with the IC_{50} values determined for rbOCT1 and rbOCT2 expressed in cultured cells (details as in Fig. 4). ○, Mean IC_{50} value ± SD for inhibition of mediated TEA uptake in isolated, single nonperfused S3 segments of rabbit RPT.

and TYR. The IC_{50} for CIM inhibition of transport was 53.6 ± 8.3 μM, whereas the IC_{50} for TYR inhibition was 2,890 ± 1,580 μM (Fig. 6*A*). These values were qualitatively consistent with those observed in the S2 segment and differed sharply from those observed in the S1 segment in that CIM was a much more effective inhibitor of TEA transport than was TYR. These data suggest, therefore, that TEA transport in the S3 segment is dominated by activity of OCT2, with comparatively little influence by OCT1 (Fig. 6*B*).

Comparative transport of TEA and amantadine in rabbit RPT. Rat RPT express a basolateral transport process that accepts the antiviral compound amantadine but is not inhibited by TEA (3). The structural characteristics of amantadine are such that it would be generally considered a type I OC, and its transport by rat OCT1 and OCT2 (2) is consistent with that view. Figure 7 confirms that amantadine also interacts with rabbit OCT1 and OCT2, inhibiting TEA transport into CHO cells that stably expressed each process with IC_{50} values of 7.1 ± 0.85 μM (n = 2) and 31.6 ± 4.2 μM (n = 3), respectively. In light of these observations, we examined amantadine's interaction with TEA transport in single isolated rabbit RPT. Figure 8 shows the time course of [^{3}H]amantadine uptake in single S2 segments. Uptake of radiolabel was time dependent over the first 30 s and approached steady state within 2 min. At the earliest time point (2 s), there was a suggestion of a rapid binding component to total amantadine accumulation, and this was supported by the observation that addition of 1.5 mM unlabeled amantadine reduced the 2-min accumulation of labeled substrate to approximately the value observed at 2 s. Figure 9 shows the effect of 1.5 mM concentrations of unlabeled TEA and amantadine on the basolateral uptake of [^{3}H]TEA and [^{3}H]amantadine. The complete block of mediated [^{3}H]TEA uptake produced by addition of the unlabeled substrates was consistent with the conclusion that basolateral TEA uptake can be accounted for by the combined influence of OCT1 and OCT2 (although, because these were S2 segments, it was likely to have been dominated by OCT2). The profile of inhibition of amantadine uptake was, however, very different. Whereas exposure to 1.5 mM unlabeled amantadine reduced uptake by 60% (with the remainder likely the result of binding; see Fig. 7), 1.5 mM TEA reduced [^{3}H]amantadine uptake by only 22%. The fraction of amantadine uptake blocked by TEA probably represents that involving interaction with OCT2 and/or OCT1, with the remaining fraction that was blocked by 1.5 mM amantadine reflecting interaction with one or more additional transport pathways.

DISCUSSION

In previous studies, we showed that basolateral TEA transport in isolated S2 segments of rabbit RPT is dominated by functional expression of OCT2 (11, 26). Our current results show that the profile of functional OCT expression changes along the length of the rabbit RPT. Assessment of functional expression of OCT1 vs. OCT2 is based on the observation that, whereas both homologs display similar affinities for TEA, they have very different affinities for selected compounds, i.e.,

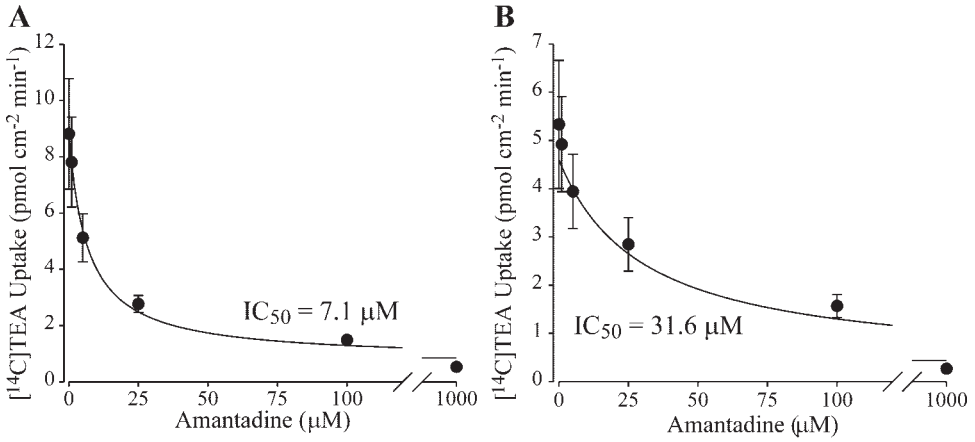

Fig. 7. Kinetics of inhibition of [^{14}C]TEA transport, mediated by rbOCT1 (*A*) or rbOCT2 (*B*), produced by increasing concentrations of amantadine. The cloned transporters were stably expressed in CHO cells, and initial rates of transport were estimated from 2-min uptakes of 12 μM [^{14}C]TEA. Each point is the mean ± SE of uptakes, each performed in triplicate, in 2 (OCT1) or 3 (OCT2) experiments.

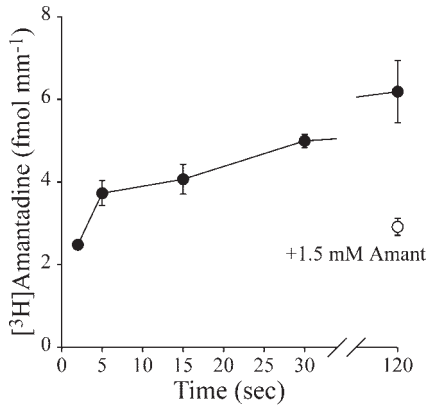

Fig. 8. Time course of [^{3}H]amantadine (Amant; 0.57 ± 0.03 μM) uptake in isolated single S2 segments of rabbit RPT. Uptakes were measured in absence or presence of 1.5 mM unlabeled amatadine. ●, Mean uptakes ± SE, measured in triplicate, in tubules from 2 different rabbits. Uptake measured in the presence of 1.5 mM amantadine (○) was measured in triplicate, in 2 experiments.

so-called "discriminating" or "homolog-specific" inhibitors (11). In the present work, functional mapping of OCT activity used the fact that rbOCT1 displays a 12- to 17-fold higher apparent affinity for TYR than does rbOCT2 and that rbOCT2 displays a 50- to 70-fold higher affinity for CIM than does rbOCT1 (11). Consequently, expression of different OCT homologs in different segments could be characterized by segment-specific profiles of TEA uptake that had *1*) similar K_t values for TEA transport but *2*) different IC_{50} values for inhibition by TYR and CIM.

Consistent with the above prediction, basolateral TEA transport into S1, S2, and S3 segments of rabbit RPT was relatively constant, with K_{50} values in the three segments of 33, 74, and 30 μM and J_{cap} values of 0.8, 0.9, and 1.2 pmol·min^{-1}·mm^{-1}, respectively. It is worth noting that rabbit OCT1 and OCT2 have sufficiently similar K_t values for TEA when expressed in COS-7 cells (120 vs. 76 μM, respectively) or CHO cells (20 vs. 35 μM, respectively; see Ref. 11) such that the parallel activity of the two processes in native RPT would behave kinetically as the single process that has frequently been assumed to account for observed OC transport (e.g., Ref. 21). The similarity of transport parameters for TEA in the three RPT segments seen here is consistent with the observation by Schäli et al. (19) of virtually identical steady-state TEA accumulation in nonperfused S1, S2, and S3 segments of rabbit RPT.

In contrast to the near-constant profile of TEA interaction with expressed OC transport in the different segments of rabbit RPT, the interaction of the homolog-specific inhibitors TYR and CIM differed markedly in the three segments. In the S2 segment, as noted previously (11) and summarized in Fig. 4, CIM was a high-affinity inhibitor (IC_{50} of 20 μM), and TYR a low-affinity inhibitor (IC_{50} of 386 μM), of basolateral TEA uptake. The quantitative characteristics of these interactions were sufficiently similar to those observed in studies of rbOCT2 (in heterologous expression systems) to support the conclusion that transport of TEA, and of other substrates that do not discriminate between OCT1 and OCT2, is dominated by functional expression of OCT2. However, in isolated S1 segments of rabbit RPT, TYR was the high-affinity inhibitor of TEA uptake (IC_{50} of 39 μM), whereas CIM was a low-affinity inhibitor (IC_{50} of 328 μM). These values are sufficiently close to those characteristic of rbOCT1 to support the conclusion that TEA transport in cells of the S1 segment of rabbit RPT is dominated by functional expression of OCT1.

TEA uptake in the S3 segment was, on the other hand, consistent with the S2 profile of high affinity for CIM and low affinity for TYR, suggestive of the influence of OCT2 rather than OCT1. Confidence in this conclusion is tempered, however, by the observation that the IC_{50} values for both inhibitors were larger than those measured for inhibition of OCT2-mediated TEA transport in either COS-7 or CHO cells, or to those measured in isolated S2 segments. The basis for the reduced inhibitory efficacy of CIM and TYR in the S3 segment is unclear. Although it could infer the influence of one or more additional pathways for TEA transport in S3 cells, it could also reflect differences in cell-specific factors that influence the characteristics of transport. That such factors exist is supported by the differences in kinetic parameters for rabbit OCT1 and OCT2 when expressed in CHO cells vs. COS-7 cells: IC_{50} values for inhibition of both transporters are routinely ~2.5 times larger when measured in COS-7 cells (11). It is unlikely that the different inhibitory profiles of S2 and S3 segments reflect the influence of OCT3 in light of the fact that the half-saturation constant for TEA in the S3 segment was similar to that observed for the S1 and S2 segments and inconsistent

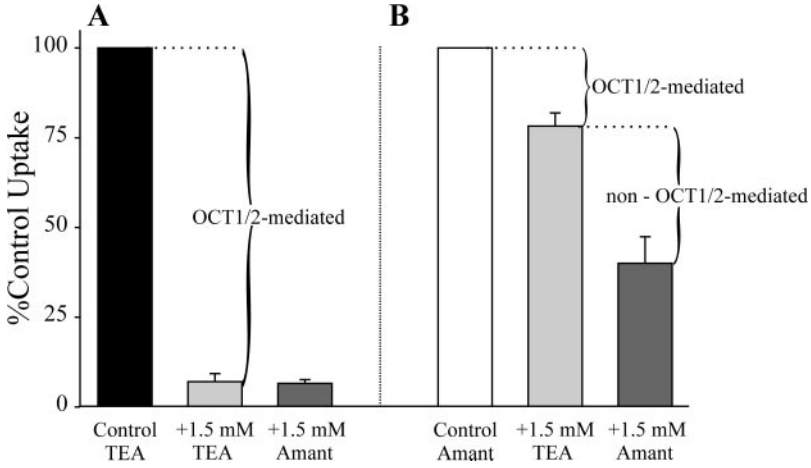

Fig. 9. *A*: inhibition of [^{3}H]TEA (0.45 ± 0.03 μM) transport in isolated, single nonperfused S2 segments of rabbit RPT produced by 1.5 mM concentrations of either unlabeled TEA or amantadine. The height of each bar represents the mean ± SE of 2-min uptakes, measured in triplicate, in tubules from 2 rabbits. *B*: inhibition of [^{3}H]amantadine (0.46 ± 0.16 μM) transport in isolated, single nonperfused S2 segments of rabbit RPT produced by 1.5 mM concentrations of either unlabeled TEA or amantadine. The height of each bar represents the mean ± SE of 2-min uptakes, measured in triplicate, in tubules from 3 rabbits.

with the very low affinity for TEA that is characteristic of OCT3 in the rat (2.5 mM; see Ref. 13) and mouse (1.9 mM; see Ref. 23).

It is interesting to compare the functional roles of OCT1 and OCT2 in rabbit RPT with the relative levels of mRNA expression of these two transporters. Consistent with results obtained in the rat (20) and human (16), expression of OCT1 mRNA in rabbit renal cortex appears to be ~10% or less than that of OCT2 (Fig. 1). Despite the apparent disparity at the mRNA level, functional expression of OCT1 appears to be great enough in rabbit kidney to have that homolog play the predominant role in basolateral TEA transport in the S1 segment of RPT. It is also noteworthy that, despite the comparatively low level of functional expression of OCT1 in the S2 segment (Fig. 4 and Refs. 11 and 26), there is sufficient OCT1 activity in S2 cells to have that homolog play the predominant role in basolateral uptake of the OCT1-selective substrate, TYR (11). Conversely, the apparent predominance of OCT1-like activity in the S1 segment of rabbit RPT should not be taken as evidence that OCT2 cannot play a quantitatively important role in the basolateral transport of OCT2-selective substrates in that segment.

Levels and patterns of expression of OCT mRNA in rat kidney also belie the apparent physiological roles of OCT1 and OCT2. Karbach et al. (12) noted that the highest level of OCT1 mRNA expression evident by in situ hybridization in rat kidney is in the outer medulla, yet immunocytochemical localization of OCT1 and OCT2 revealed the former to be restricted to the S1 and S2 region of rat RPT, whereas the latter was expressed in the S2 and S3 segments. Although neither of these techniques provides evidence concerning levels of functional expression of transport activity, the apparent distribution of OCT1 and OCT2 transport protein in rat kidney appears to parallel the functional distribution of OCT1 and OCT2 transport activity in rabbit kidney. Real-time PCR analysis of RNA from samples of human renal tissue found OCT1 mRNA expression to be ~1% that of OCT2, and Western blot analysis failed to observe OCT1 in crude membranes from human kidney (16). Although these data suggest that OCT1 may play little if any role in OC secretion in human kidney, such a conclusion may be premature. The profile of OCT1 function in rabbit RPT indicates that comparatively low levels of expression may, nevertheless, result in physiologically significant levels of activity, and the same may be true in human RPT.

Amantadine transport in rat RPT has been shown to involve processes distinct from either OCT1 or OCT2 (2). Despite the fact that amantadine is a substrate for the rat homologs of both of these transporters (2), uptake of amantadine in rat RPT is not reduced significantly by the presence of exogenous TEA (3). Although there is evidence for at least two kinetically distinct pathways in rat RPT (3), the majority of amantadine uptake in rat RPT involves a high-affinity/high-capacity amantadine pathway notable for its sensitivity to bicarbonate and its insensitivity to TEA (3). In the present study, we showed that amantadine interacts effectively with rabbit OCT1 and OCT2 and is transported in isolated rabbit RPT. We also found that a concentration of TEA capable of completely eliminating OCT1- and OCT2-mediated transport did not eliminate uptake of amantadine. However, in contrast to results obtained with isolated rat RPT, exogenous TEA was capable of significantly reducing amantadine accumulation in rabbit RPT (Fig. 9). Presumably, the fraction of amantadine accumulation blocked by TEA represented the portion of total amantadine uptake that occurred via OCT1 and/or OCT2, suggesting a significant role for these processes in the uptake of amantadine (and TEA). The relative inhibitory effectiveness of TEA may also reflect the observation that the rate of amantadine transport in rabbit RPT, relative to that of TEA, is lower than observed in the rat, suggesting a lower (relative) expression of the non-OCT1/2 pathway(s) in the rabbit. Nevertheless, the evidence for the significant presence of at least one additional pathway for type I OCs in the basolateral membrane of rabbit RPT underscores the complexity of the molecular organization of renal OC secretion.

In summary, the present results showed a heterogeneous distribution of transport activity mediated by the two homologous OC transporters, OCT1 and OCT2, along the length of the rabbit RPT. OCT1, despite the presence of comparatively low levels of its mRNA, appeared to be the predominant basolateral pathway for uptake of TEA (and, presumably, other type I OCs) in cells of the S1 segment of rabbit RPT. In contrast, the S2 and S3 segments displayed a pattern of substrate interaction consistent with service of OCT2 as the predominant pathway for accumulation of TEA. However, the inability of TEA to eliminate mediated uptake of the type I substrate, amantadine, in isolated S2 segments indicated that basolateral OC transport can involve the concerted activity of at least one process in addition to OCT1 and OCT2.

GRANTS

This work was supported in part by National Institutes of Health Grants DK-58251, ES-04940, ES-06694, and HL-07249 and by Canadian Institutes of Health Research Grant ROP14710.

REFERENCES

1. **Bednarczyk D, Mash EA, Aavula BR, and Wright SH.** NBD-TMA: a novel fluorescent substrate of the peritubular organic cation transporter of renal proximal tubules. *Pflügers Arch* 440: 184–192, 2000.
2. **Goralski KB, Lou G, Prowse MT, Gorboulev V, Volk C, Koepsell H, and Sitar DS.** The cation transporters rOCT1 and rOCT2 interact with bicarbonate but play only a minor role for amantadine uptake into rat renal proximal tubules. *J Pharmacol Exp Ther* 303: 959–968, 2002.
3. **Goralski KB and Sitar DS.** Tetraethylammonium and amantadine identify distinct organic cation transporters in rat renal cortical proximal and distal tubules. *J Pharmacol Exp Ther* 290: 295–302, 1999.
4. **Gorboulev V, Ulzheimer JC, Akhoundova A, Ulzheimer-Teuber I, Karbach U, Quester S, Baumann C, Lang F, Busch AE, and Koepsell H.** Cloning and characterization of two human polyspecific organic cation transporters. *DNA Cell Biol* 16: 871–881, 1997.
5. **Groves CE, Evans K, Dantzler WH, and Wright SH.** Peritubular organic cation transport in isolated rabbit proximal tubules. *Am J Physiol Renal Fluid Electrolyte Physiol* 266: F450–F458, 1994.
6. **Gründemann D, Gorboulev V, Gambaryan S, Veyhl M, and Koepsell H.** Drug excretion mediated by a new prototype of polyspecific transporter. *Nature* 372: 549–552, 1994.
7. **Gründemann D, Schechinger B, Rappold GA, and Schomig E.** Molecular identification of the corticosterone-sensitive extraneuronal catecholamine transporter. *Nat Neurosci* 1: 349–351, 1998.
8. **Hartley DP and Klaassen CD.** Detection of chemical-induced differential expression of rat hepatic cytochrome P450 mRNA transcripts using branched DNA signal amplification technology. *Drug Metab Dispos* 28: 608–616, 2000.
9. **Holohan PD and Ross CR.** Mechanisms of organic cation transport in kidney plasma membrane vesicles: 2. ΔpH studies. *J Pharmacol Exp Ther* 216: 294–298, 1981.
10. **Jonker JW, Wagenaar E, Van Eijl S, and Schinkel AH.** Deficiency in the organic cation transporters 1 and 2 (Oct1/Oct2 [Slc22a1/Slc22a2]) in

mice abolishes renal secretion of organic cations. *Mol Cell Biol* 23: 7902–7908, 2003.
11. **Kaewmokul S, Chatsudthipong V, Evans KK, Dantzler WH, and Wright SH.** Functional mapping of rbOCT1 and rbOCT2 activity in the S2 segment of rabbit proximal tubule. *Am J Physiol Renal Physiol* 285: F1149–F1159, 2003.
12. **Karbach U, Kricke J, Meyer-Wentrup F, Gorboulev V, Volk C, Loffing-Cueni D, Kaissling B, Bachmann S, and Koepsell H.** Localization of organic cation transporters OCT1 and OCT2 in rat kidney. *Am J Physiol Renal Physiol* 279: F679–F687, 2000.
13. **Kekuda R, Prasad PD, Wu X, Wang H, Fei YJ, Leibach FH, and Ganapathy V.** Cloning and functional characterization of a potential-sensitive, polyspecific organic cation transporter (OCT3) most abundantly expressed in placenta. *J Biol Chem* 273: 15971–15979, 1998.
14. **Meijer DKF, Mol WEM, Müller M, and Kurz G.** Carrier-mediated transport in the hepatic distribution and elimination of drugs, with special reference to the category of organic cations. *J Pharmacokinet Biopharm* 18: 35–70, 1990.
15. **Meyer-Wentrup F, Karbach U, Gorboulev V, Arndt P, and Koepsell H.** Membrane localization of the electrogenic cation transporter rOCT1 in rat liver. *Biochem Biophys Res Commun* 248: 673–678, 1998.
16. **Motohashi H, Sakurai Y, Saito H, Masuda S, Urakami Y, Goto M, Fukatsu A, Ogawa O, and Inui K-I.** Gene expression levels and immunolocalization of organic anion transporters in the human kidney. *J Am Soc Nephrol* 13: 866–874, 2002.
17. **Okuda M, Saito H, Urakami Y, Takano M, and Inui K-I.** cDNA cloning and functional expression of a novel rat kidney organic cation transporter, OCT2. *Biochem Biophys Res Commun* 224: 500–507, 1996.
18. **Rennick B.** Renal tubule transport of organic cations. *Am J Physiol Renal Fluid Electrolyte Physiol* 240: F83–F89, 1981.
19. **Schäli C, Schild L, Overney J, and Roch-Ramel F.** Secretion of tetraethylammonium by proximal tubules of rabbit kidneys. *Am J Physiol Renal Fluid Electrolyte Physiol* 245: F238–F246, 1983.
20. **Slitt AL, Cherrington NJ, Hartley DP, Leazer TM, and Klaassen CD.** Tissue distribution and renal developmental changes in rat organic cation transporter mRNA levels. *Drug Metab Dispos* 30: 212–219, 2002.
21. **Ullrich KJ, Papavassiliou F, David C, Rumrich G, and Fritzsch G.** Contraluminal transport of organic cations in the proximal tubule of the rat kidney. I. Kinetics of N^1-methylnicotinamide and tetraethylammonium, influence of K^+, HCO_3, pH; inhibition by aliphatic primary, secondary and tertiary amines, and mono- and bisquaternary compounds. *Pflügers Arch* 419: 84–92, 1991.
22. **Wright SH and Dantzler WH.** Molecular and cellular physiology of renal organic cation and anion transport. *Physiol Rev* In press.
23. **Wu X, Huang W, Ganapathy ME, Wang H, Kekuda R, Conway SJ, Leibach FH, and Ganapathy V.** Structure, function, and regional distribution of the organic cation transporter OCT3 in the kidney. *Am J Physiol Renal Physiol* 279: F449–F458, 2000.
24. **Zhang L, Brett CM, and Giacomini KM.** Role of organic cation transporters in drug absorption and elimination. *Annu Rev Pharmacol Toxicol* 38: 431–460, 1998.
25. **Zhang L, Dresser MJ, Gray AT, Yost SC, Terashita S, and Giacomini KM.** Cloning and functional expression of a human liver organic cation transporter. *Mol Pharmacol* 51: 913–921, 1997.
26. **Zhang X, Evans KK, and Wright SH.** Molecular cloning of rabbit organic cation transporter rbOCT2 and functional comparisons with rbOCT1. *Am J Physiol Renal Physiol* 283: F124–F133, 2002.